SMART BATTERY MANAGEMENT SYSTEM USING PIC MICROCONTROLLER

[1]Ranjit Govind Ganage, [2]Rohit Rajkumar Kumbhar, [3]Pratik Dattatray Parchande
[123]B.Tech Student, Department of Electronics & Telecommunication Engineering
Karmayogi Institute of Technology, Pandharpur, Maharashtra, India
Dr. Babasaheb Ambedkar Technological University, Lonere
Project Guide: *Dr. S. M. Lambe, HOD, Department of Electronics & Telecommunication Engineering*

Abstract**—***This paper presents a Smart Battery Management System (SBMS) designed using the PIC18F4520 microcontroller for monitoring and protecting lithium-ion (Li-ion) batteries. The system continuously acquires three key battery parameters—voltage, current, and temperature—using a resistive voltage divider, an ACS712-20A Hall-effect current sensor, and an LM35 precision temperature sensor, respectively. The microcontroller processes the analog signals through its onboard 10-bit Analog-to-Digital Converter (ADC) and enforces firmware-defined protection thresholds. When the battery voltage falls below 3.3 V, a MOSFET-controlled charging circuit is activated; when it reaches or exceeds 3.3 V, charging is disconnected to prevent overcharging. When the battery temperature reaches or exceeds 35°C, a DC cooling fan is activated for thermal management. All parameters are displayed in real time on a 16×2 LCD module. Experimental results confirm accurate parameter measurement and reliable protection actuation, demonstrating a cost-effective solution (total BOM: ₹1,468) suitable for small-scale battery management in renewable energy and portable device applications.*

Keywords**—***Battery Management System; PIC18F4520; ACS712; LM35; MOSFET; lithium-ion battery; voltage divider; LCD display; overcharge protection; thermal management.*

I. INTRODUCTION

The proliferation of battery-powered technologies—electric vehicles, solar energy storage systems, and portable consumer electronics—has created an acute demand for reliable, intelligent battery management. Lithium-ion (Li-ion) batteries dominate these applications owing to their high energy density, low self-discharge rate, and long service life. However, Li-ion cells are chemically sensitive and must operate within well-defined voltage and temperature windows. Overcharging raises internal pressure, degrades the electrolyte, and can initiate thermal runaway; excessive heat during charging accelerates capacity fade and may cause permanent cell damage. Without active supervision, conventional charging circuits cannot guarantee compliance with these constraints [1].

A Battery Management System (BMS) addresses these issues by continuously monitoring battery state variables and enforcing safety limits through actuator control. Despite widespread research interest, BMS designs targeting small-scale or educational platforms either employ external ADC modules that inflate cost and board area, or use fixed-threshold analog comparators that lack firmware configurability [2], [3]. This paper presents a fully embedded, single-chip SBMS that integrates all signal acquisition, conversion, protection logic, and actuation within a PIC18F4520 microcontroller, achieving a compact and low-cost design without sacrificing flexibility.

The remainder of this paper is organised as follows. Section II reviews related work. Section III describes the hardware and firmware architecture. Section IV presents experimental results. Section V concludes and outlines future work.

II. LITERATURE REVIEW

Gabbar et al. [1] surveyed global BMS architectures and standards, establishing voltage, current, and temperature monitoring as the three mandatory pillars of battery protection. Patel [2] analysed microcontroller-driven BMS topologies, showing that embedded ADC acquisition with real-time decision loops offers the best tradeoff between response latency and cost. Ramesh and Gupta [3] implemented a microcontroller-based voltage-and-temperature monitor that automatically disconnects charging at a preset threshold—an approach that directly inspired the MOSFET cut-off logic in this work. Kıvrak et al. [4] demonstrated that N-channel enhancement-mode MOSFETs provide low conduction-loss switching ideal for compact BMS protection circuits. Wibowo [5] characterised the ACS712 Hall-effect sensor for DC current monitoring, including offset calibration and noise suppression relevant to battery applications. Winanta et al. [8] integrated all three sensor types with LCD display and fan-based cooling—a configuration closely aligned with the system presented here. Collectively, the literature supports a single-chip, firmware-configurable architecture as a practical and reproducible approach to low-cost BMS design.

III. SYSTEM DESIGN

A. System Architecture

The SBMS comprises six functional blocks: (i) the Li-ion battery under test; (ii) the analog sensing front end (voltage divider, ACS712, LM35); (iii) the PIC18F4520 microcontroller with onboard 10-bit ADC; (iv) the MOSFET-based charging switch; (v) the transistor-driven DC cooling fan; and (vi) a 16×2 HD44780-compatible LCD display. A regulated 5 V DC rail derived from a

230 VAC–12 VAC transformer, a full-wave bridge rectifier, and a 7805 linear voltage regulator supplies all low-voltage circuitry. The microcontroller executes a closed-loop polling routine: all three sensor channels are read sequentially through the ADC, compared against firmware-defined thresholds, protection outputs are updated, and the LCD is refreshed before the cycle repeats.

B. Voltage Sensing

The Li-ion cell voltage (2.5 V–4.2 V nominal) is stepped down by a 47 kΩ–10 kΩ resistive voltage divider (division ratio ≈0.175) before being applied to ADC channel AN0. The firmware recovers the actual battery voltage using an empirically calibrated multiplier of ×11. The 10-bit ADC with a 5 V reference yields a least-significant-bit weight of 5/1023 ≈4.89 mV. The firmware charging cut-off threshold is 3.3 V: the MOSFET gate is driven HIGH (charging ON) when the computed voltage is below 3.3 V, and LOW (charging OFF) when it equals or exceeds 3.3 V, thereby preventing overcharging.

C. Current Sensing

The ACS712ELCTR-20A Hall-effect sensor (range: ±20 A, sensitivity: 100 mV/A, quiescent output: 2.5 V) is connected in series with the battery charge path and its output is sampled on AN1. The firmware computes the current as: $I = (V_{out} - 2.5) / 0.1$, where V_{out} is the ADC-reconstructed sensor output voltage. The signed result distinguishes charge (positive) from discharge (negative) current. Small negative readings near −0.02 A observed at rest reflect the quiescent load of the microcontroller circuitry drawing from the cell.

D. Temperature Sensing and Fan Control

The LM35 precision temperature sensor provides a linear output of 10 mV/°C, connected to ADC channel AN2. The firmware converts the ADC reading to a voltage, then multiplies by 100 to obtain temperature in degrees Celsius. When the computed temperature reaches or exceeds 35°C, the microcontroller activates a DC cooling fan through a BC547 NPN transistor. Below 35°C the fan is de-energised to conserve power. The LM35 requires no external calibration and offers ±0.5°C typical accuracy, ensuring repeatable threshold detection.

E. Microcontroller and Firmware

The PIC18F4520 (Microchip Technology) is an 8-bit RISC device with 32 KB Flash, 1.5 KB SRAM, 256 bytes EEPROM, and a 10-bit SAR ADC with 13 multiplexed input channels. Operating at 4 MHz from an external crystal, it yields a 1 µs instruction cycle. Port B drives the LCD in 8-bit mode; Port D supplies LCD control lines (RS, R/$\overline{W}$, EN) and the fan drive signal; Port C carries the MOSFET gate drive. Firmware is developed in Embedded C using Microchip XC8 compiler under MPLAB X IDE. The ADC is configured right-justified with $F_{osc}/32$ clock, satisfying the minimum 1.6 µs T_{AD} requirement at 4 MHz per DS39897D, and a 12 T_{AD} acquisition time to allow channel settling before conversion. The main loop samples AN0→AN1→AN2 sequentially, applies conversion formulas, updates the LCD, and drives all protection outputs.

F. Component Specifications

Table 1: Bill of Material

No.	Component	Key Specification	Qty	Cost (INR)
1	PIC18F4520	8-bit MCU, 40 MHz, 10-bit ADC	1	443
2	Crystal Oscillator	4 MHz, 22 pF load caps	1	15
3	ACS712-20A	Hall-effect, ±20 A, 100 mV/A	1	90
4	LM35	10 mV/°C, 4–30 V supply	1	90
5	LCD 16×2	HD44780 controller, 5 V DC	1	120
6	2N7000 MOSFET	N-ch enhancement, 60 V, 200 mA	4	200
7	BC547 Transistor	NPN BJT, 45 V, 100 mA	1	20
8	7805 Regulator	Fixed +5 V, 1 A output	1	15
9	Transformer	230 V / 12 V, 500 mA	1	120
10	DC Cooling Fan	5 V DC	1	150
11	Li-ion Cell	3.7 V, 4 Ah	1	100
12	Miscellaneous	Resistors, capacitors, diodes, PCB	—	105
—	—	—	Total	1,468

IV. RESULTS AND DISCUSSION

The assembled prototype was powered from a 230 V AC mains supply through the transformer-rectifier-regulator chain. All three measurement channels were verified independently before system-level characterisation.

A. Voltage Measurement and Charging Control

Fig. 1 shows the LCD output when the measured battery voltage (2.796 V) is below the 3.3 V threshold: the firmware correctly activates the charging MOSFET and displays “Start charging.” Fig. 2 shows the response at 3.710 V, which exceeds the threshold: the MOSFET is switched off and the LCD reads “Cut off power.” The state transition was observed to be stable with no hysteresis-related chatter, confirming reliable threshold detection.

Fig. 1: V = 2.796 V – charging active

Fig. 2: V = 3.710 V – charging cut off

B. Current Measurement

Fig. 3 shows the current reading during a battery rest condition. The ACS712 output settled close to its quiescent mid-rail voltage (2.5 V), yielding a computed current of −0.017 A. This small negative offset is consistent with the quiescent supply current drawn by the microcontroller and peripheral circuitry from the cell. The signed-current capability of the ACS712 correctly differentiates the charge and discharge conditions.

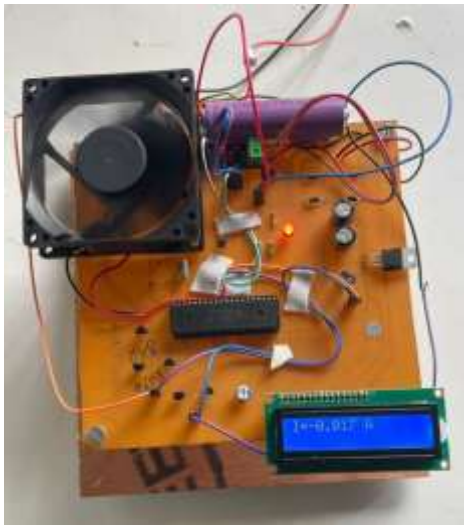

Fig. 3: Current measurement – I = −0.017 A (battery rest condition)

C. Temperature Measurement and Fan Control

Figs. 4 and 5 demonstrate the thermal management subsystem. At 29.3°C (below the 35°C threshold) the fan is inactive ("Stop rotating"). At 36.2°C the firmware immediately activates the cooling fan ("Start rotating"). The LM35 (±0.5°C accuracy, no calibration required) ensures repeatable threshold detection.

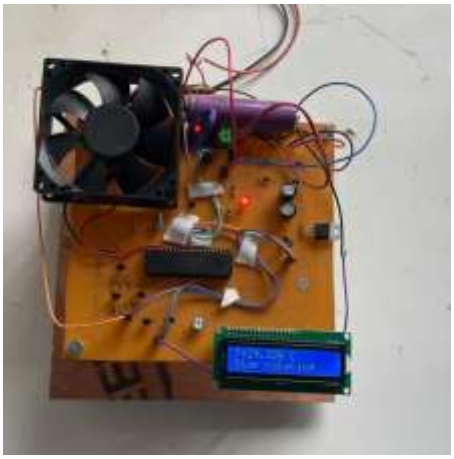

Fig. 4: T = 29.3°C – fan off (stop rotating)

Fig. 5: T = 36.2°C – fan on (start rotating)

D. Overall System Performance

Fig. 6 shows the assembled prototype in operating condition, connected to the 230 V AC mains supply. The 16×2 LCD is clearly readable under normal lighting, the charge-status LED indicator is visible, and the DC fan is mounted on the wooden substrate adjacent to the PCB. Table 2 compares measured performance against design targets across all key parameters.

Fig. 6: Assembled SBMS prototype in operating condition

Table 2: System Performance Summary

Parameter	Design Target	Measured / Achieved	Status
Voltage threshold	3.3 V	3.3 V (firmware)	✓ Met
ADC resolution	< 50 mV / LSB	≈4.89 mV / LSB	✓ Met
Temperature threshold	35°C	35°C (firmware)	✓ Met
Temperature accuracy	±1°C	±0.5°C (LM35)	✓ Met
Current direction detect	Bidirectional	Yes (signed ACS712)	✓ Met
LCD update period	Real-time	~3 s / cycle	✓ Met
Total BOM cost	< ₹2,000	₹1,468	✓ Met

V. CONCLUSION

This paper has presented and experimentally validated a compact, low-cost Smart Battery Management System built around the PIC18F4520 microcontroller. The system monitors battery voltage via a resistive divider, current via an ACS712-20A Hall-effect sensor, and temperature via an LM35 precision sensor, enforcing a 3.3 V cut-off threshold for overcharge protection and a 35°C activation threshold for fan-based cooling. Real-time parameter display on a 16×2 LCD provides clear operational feedback. Experimental results confirm that all protection actions engage and disengage reliably at the configured thresholds, and the total bill of materials cost (₹1,468) is substantially lower than commercially available BMS modules of equivalent functionality.

Future enhancements will target three areas: (i) interrupt-driven ADC sampling to reduce loop latency and enable firmware sleep modes for power saving; (ii) a Coulomb-counting algorithm to estimate State of Charge (SoC) in real time; and (iii) integration of a wireless interface (Bluetooth / Wi-Fi) to support remote monitoring via a mobile application, extending the platform toward IoT-enabled battery management for electric vehicle and solar energy storage deployments.

REFERENCES

[1] H. A. Gabbar et al., "Review of Battery Management Systems (BMS) Development and Standards," Technologies, vol. 9, no. 3, pp. 1–21, 2021.

[2] A. Patel, "Microcontroller-Driven Battery Management in Hybrid Energy Systems—A Systematic Review," ResearchGate, 2022.

[3] S. Ramesh and P. Gupta, "Battery Management System using Microcontroller," Int. J. Research in Engineering and Technology, vol. 9, no. 2, pp. 45–50, 2020.

[4] A. Kıvrak et al., "Battery Management System Implementation with Passive Control using MOSFET," SAGE Open, vol. 13, no. 1, 2023.

[5] Y. Wibowo, "Design of ACS712-Based Current Sensing Monitoring System," UNNES J. Electrical Engineering, vol. 13, no. 4, pp. 210–217, 2024.

[6] D. Singh and A. Kumar, "True RMS Current Measurement using ACS712 in Power Electronics," ResearchGate, 2022.

[7] J. Lee and S. Park, "Design and Implementation of a Battery Overcharge Protection Circuit," IEEE Conf. Proc., 2024.

[8] G. Winanta et al., "Design and Construction of Protection and Monitoring System for Batteries," AIP Conf. Proc., vol. 2720, 2023.

[9] R. Das, "An Efficient Battery Management System for Series Connected Li-ion Pack," IJAREEIE, vol. 9, no. 8, pp. 987–993, 2020.

[10] A. Haldar et al., "IoT-Enabled Advanced Monitoring System for Tubular Batteries," Energy Reports, vol. 12, pp. 324–333, 2024.

[11] S. Karthik et al., "Analysis of Cell Balancing of Li-Ion Batteries with Dissipative Balancing," J. Energy Storage, vol. 72, 2024.

[12] N. Sharma and A. Jain, "A Review on Battery Health Monitoring System," IJERA, vol. 13, no. 2, pp. 65–72, 2023.